*Journal of Applied Electrochemistry* **31**: 1079–1087, 2001.



# Corrosion of Au–Pd–In alloy in simulated physiological solutions

K. LEINARTAS[1], P. MIEČINSKAS[1], A. SUDAVIČIUS[1], D. JELINSKIENĖ[1], R. JUŠKĖNAS[1], V. LISAUSKAS[2], B. VENGALIS[2] and E. JUZELIŪNAS[1]*
[1]*Institute of Chemistry, A. Goštauto 9, 2600 Vilnius, Lithuania*
[2]*Semiconductor Physics Institute, A. Goštauto 12, 2600 Vilnius, Lithuania,*
*(*author for correspondence, fax: (3702) 617018, e-mail: ejuzel@ktl.mii.lt)*

Received 28 February 2001; accepted in revised form 15 May 2001

*Key words:* corrosion, dental alloys, EQCM, gold alloys, magnetron sputtering, nanogravimetry

**Abstract**

The corrosion of Au–Pd–In alloy, which is of great importance in dentistry, has been studied using an electrochemical quartz crystal microbalance (EQCM) in simulated physiological solutions. The alloy was deposited on quartz substrates by means of magnetron sputtering (MS). Analysis performed using X-ray photoelectron spectroscopy showed that the chemical composition of the sputtered deposit was similar to that of the MS target made of conventional casting alloy. Investigations by X-ray diffraction indicated a crystalline structure of the MS alloy. The electrochemical and corrosion behaviour of the Au–Pd–In alloy was studied in three simulated physiological solutions: 0.9 M NaCl, 0.1 M NaCl + 0.1 M lactic acid and artificial saliva. Determination of break down potential was complicated by the anodic gold dissolution due to formation of a chloride complex. The onset of anodic currents, therefore, indicated not the potential at which the passive layer starts to be destroyed, but the exceeding of the $Au/AuCl_4^-$ equilibrium potential, which does not directly reflect corrosion resistance. The EQCM measurements under open circuit conditions indicated corrosion as an increase in mass, caused by the accumulation of corrosion products on the alloy surface. The increase in mass in acidic solution (pH 2.2) was similar to that in neutral solution (pH 6.5), which implies dissolution of corrosion products to be insignificant.

## 1. Introduction

Au–Pd–In alloys are widely used in medical practice, especially in dentistry. Due to good biocompatibility, high corrosion resistance and ease of casting and soldering the gold-based alloys are used to produce artificial joints, crowns, bridges and fillings in dentistry. In pathologic states, body fluids can be slightly acidic (pH 5.3–5.6), and so represent a corrosive environment [1]. Moreover, various components of body fluids, such as chloride ions, proteins, amino acids, dissolved oxygen and microorganisms may affect the metal surface state and reduce the corrosion resistance of implants. Due to *in vivo* corrosion, the functionality of implants may decrease and, furthermore, the release of metal ions into the organism may cause allergic reactions, tissue irritation etc.

To predict material resistance to *in vivo* corrosion, these materials are usually studied in artificial physiological solutions by using electrochemical methods. Thus, the corrosion potential, the breakdown potential, the rest potential and the polarization resistance have been used to assess the corrosion resistance of gold-based alloys [2–4].

The selection of electrochemical criteria for metallic biomaterials testing is often complicated. It has been shown that the impedance spectra in a low frequency domain did not always exhibit a clear resistive behaviour from which the polarization resistance could be derived and the corrosion current calculated [5–7]. Moreover, biomaterials in simulated physiological solutions often failed to exhibit clear Tafel regions, from which the corrosion current could be obtained. Another commonly used method is the determination of breakdown potentials [2–4]; however, as will be shown, application of this method to gold alloys in physiological solutions is complicated by anodic gold dissolution due to formation of a complex with chloride.

An effective alternative in corrosion testing of gold-based alloys is electrochemical quartz crystal microgravimetry (EQCM). Advantages of the method include the nanogram resolution for mass changes, the continuous information (i.e., the rate of mass change at any practical time interval) and the possibility to perform experiments in both gaseous and liquid environments. In this work an attempt has been made to apply EQCM to corrosion studies of Au–Pd–In alloy in artificial physiological solutions. The greatest difficulty in the use of EQCM as a corrosion sensor arises from coating the quartz with an alloy film, whose physical-chemical properties and, consequently, corrosive behaviour does

not differ greatly from the cast specimen. This problem has been solved in this work by using magnetron-sputtering (MS) technique.

## 2. Experimental details

The target for magnetron sputtering was made from commercially available Au–Pd–In casting alloy (BegoCer®G), whose exact composition is given in Table 1. The vacuum in the magnetron-sputtering chamber was maintained at $10^{-6}$ mm Hg. Working gas was Ar and its pressure was maintained at 0.1–0.2 Pa. The temperature in the chamber was about 100 °C. The Ar ionization current was 60 mA and the voltage was 600 V. The sputtering duration was 6–8 min, which corresponded to a coating thickness of about 0.15 $\mu$m. The set up of magnetron-sputtering apparatus and more details about the MS procedure used are given elsewhere [7, 8].

The coating composition was analysed by X-ray photoelectron spectroscopy (XPS) using surface etching by ionised argon. The spectra were recorded by an Escalab MK spectrometer (Great Britain) using X-radiation of Mg$K_\alpha$ (1253.6 eV, pass energy of 20 eV). The samples were etched in the preparation chamber by ionized argon at a vacuum of $5 \times 10^{-4}$ Pa. An accelerating voltage of about 15 kV and a beam current of 20 $\mu$A cm$^{-2}$ were used. Etching was performed at a current of 100 $\mu$A, which corresponded to an etching rate of about 20 nm min$^{-1}$. The data on binding energies were from [9, 10].

The EQCM experimental device was analogous to that described in [11]. Quartz discs (AT plane) were used, their fundamental frequency being $f_0 = 5$ MHz and radius $r = 15$ mm (produced by KVG Quartz Crystal Technology GmbH, Germany). Both quartz sides were plated with the same alloy; the coatings acted as excitation electrodes in the oscillation circuit. The crystals were mounted in a special window of a Teflon cell, with one of the sides being exposed to the solution compartment and the other one facing air. The actual electrode area, which contacted the solution, was 0.78 cm$^2$. The EQCM measurements were started several seconds after the cell had been filled with solution.

Experiments were performed in the solutions recommended for metallic biomaterials testing by standards DIN 50905, DIN EN ISO 1562 and AFNOR S 90-701, respectively: (i) 0.9 M NaCl, (ii) 0.1 M NaCl + 0.1 M lactic acid, and (iii) artificial saliva (g l$^{-1}$): $Na_2HPO_4$ – 0.26; NaCl – 0.67; KSCN – 0.33; $KH_2PO_4$ – 0.2; $NaHCO_3$ – 1.5; KCl – 1.2. These solutions were prepared using reagents of analytical grade purity and triply distilled water.

In some experiments the BegoCer®G alloy disc was used as the working electrode (the chemical composition is given in Table 1). The electrode surface was polished by an abrasive SiC paper (grade 1000), rinsed with alcohol and water, dried under ambient conditions and mounted in the window of the cell for EQCM measurements described above. The actual area of the electrode was 0.78 cm$^2$.

A saturated Ag/AgCl electrode was used as the reference electrode, and all potentials in this paper were referred to that electrode. A platinum foil served as a counter electrode. The solutions were deoxygenated by using Ar (99.99).

Voltammetric measurements were conducted by a PS-305 potentiostat (Elchema, USA) and a IM6 apparatus (Zahner, Germany).

*Table 1.* Compositions (in wt %) of the Au–Pd–In target and the alloy deposited on quartz crystal by magnetron sputtering. (Samples were analysed by XPS after surface sputtering by ionized argon)

| Depth/nm | Au | Pd | In | Ru | Ga |
|---|---|---|---|---|---|
| | *Target*/% | | | | |
| 10 | 52 | 39.7 | 6.8 | 0.3 | 1.2 |
| | *Deposit*/% | | | | |
| 1 | 62.0 | 26.4 | 10.0 | 0.17 | 1.47 |
| 10 | 53.2 | 39.1 | 6.7 | 0.14 | 0.93 |

## 3. Results and discussion

### 3.1. *Voltammetric investigations*

Figure 1 shows the cyclic voltammogram for Au–Pd–In in the solution containing 0.1 M NaCl + 0.1 M lactic acid (pH 2.3). When sweeping the potential in the positive direction, the electrode exhibits a passive behaviour in the region $E = 0$–0.8 V. At higher potentials, the anodic current appears with a peak at about 1.4 V. The peak height increased both with the chloride concentration and with the potential sweep rate (the

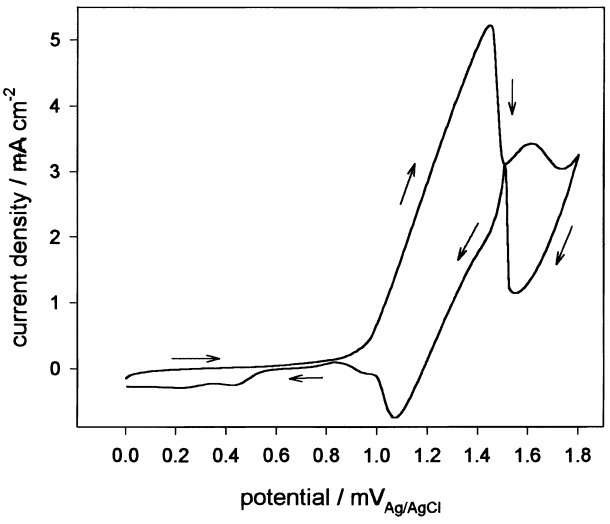


*Fig. 1.* Cyclic voltammogram recorded for Au–Pd–In alloy in the solution 0.1 M NaCl + 0.1 M lactic acid (pH 2.3). Potential sweep rate 10 mV s$^{-1}$.

data are not shown in this paper). Similar voltammetric behaviour was also observed in the solution without lactic acid, that is, in 0.1 M NaCl adjusted to pH 2.2 using HCl (Figure 2).

Figure 3 shows the cyclic voltammogram obtained for pure gold electrode (99.99%). The anodic current appears above 0.8 V, that is, in the same region as in the case of the alloy (Figures 1 and 2). This current decreases sharply above 1.5 V, that is, in the region where, according to the reverse curve, noticeable water decomposition starts. It was previously shown that the current peak under discussion was actually independent of the solution pH and it disappeared in the chloride-free solution [12]. Most likely, the current peak should be attributed to gold dissolution reactions [13]:

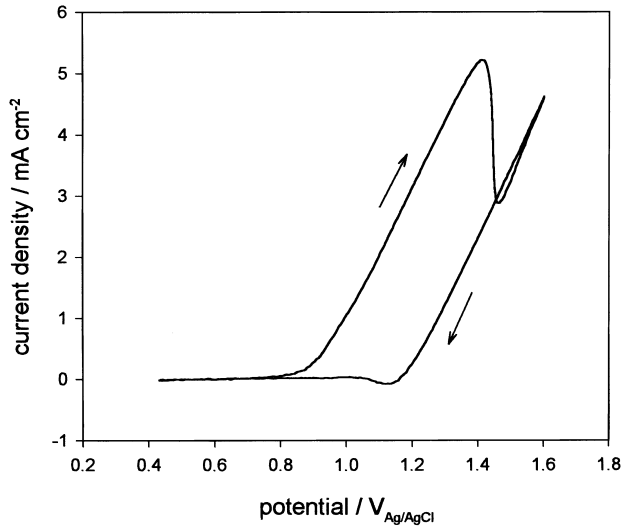


*Fig. 2.* Cyclic voltammogram recorded for Au–Pd–In alloy in 0.1 M NaCl adjusted to pH 2.2. Potential sweep rate 10 mV $s^{-1}$.

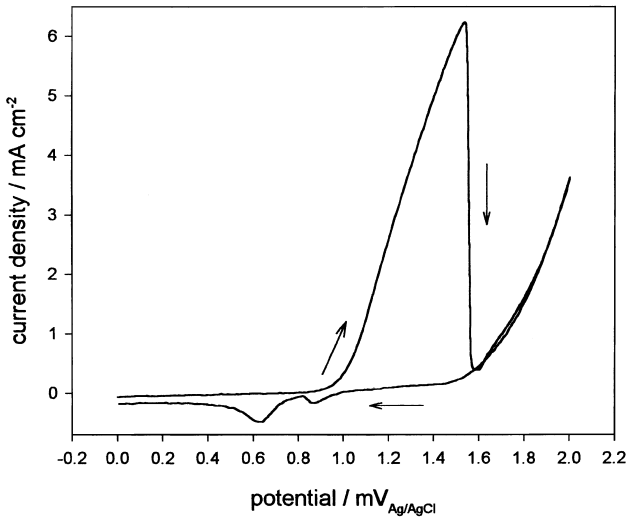


*Fig. 3.* Cyclic voltammogram recorded for pure Au electrode in 0.1 M NaCl adjusted to pH 2.2. Potential sweep rate 10 mV $s^{-1}$.

$$Au + 2\,Cl^- \rightarrow AuCl_2^- + e^{-1}$$
$$E^\circ = 0.95\,V \text{ vs } Ag/AgCl \quad (1)$$

$$Au + 4\,Cl^- \rightarrow AuCl_4^- + 3e^-$$
$$E^\circ = 0.8\,V \text{ vs } Ag/AgCl \quad (2)$$

Gold dissolution was confirmed by the EQCM measurements which showed a distinctive decrease in the electrode mass above 0.8 V [12]. It was also concluded that the appearance of the anodic peak (hysteresis) is the result of the gold dissolution inhibition by the formation of a gold oxide layer. Small cathodic peaks on the reverse curve in Figure 3 may be attributed to the reduction of gold oxide formed on the gold surface during the positive potential scan.

The onset of the anodic current at $E \geqslant 0.8$ V is characteristic of both pure gold (Figure 3) and alloy (Figures 1 and 3) electrodes. It is reasonable, therefore, to assume that gold dissolution and chloride complex formation begins above 0.8 V (Equation 2). The role of chloride as a gold dissolution agent was also confirmed by the experiments carried out in a chloride free solution adjusted to pH 2.3 (Figure 4). Obviously, there is no anodic current under discussion in this solution. At a higher pH, two current peaks at about 0.7 and 1.1 V have been observed (Figure 4). Using standard potentials as criteria, we can assume that the following reactions take place [13]:

$$Pd + H_2O \rightarrow PdO + 2\,H^+ + 2\,e^-$$
$$E^\circ = 0.65\,V \text{ vs } Ag/AgCl \quad (3)$$

$$PdO + H_2O \rightarrow PdO_2 + 2\,H^+ + 2\,e^-$$
$$E^\circ = 1.063\,V \text{ vs } Ag/AgCl \quad (4)$$

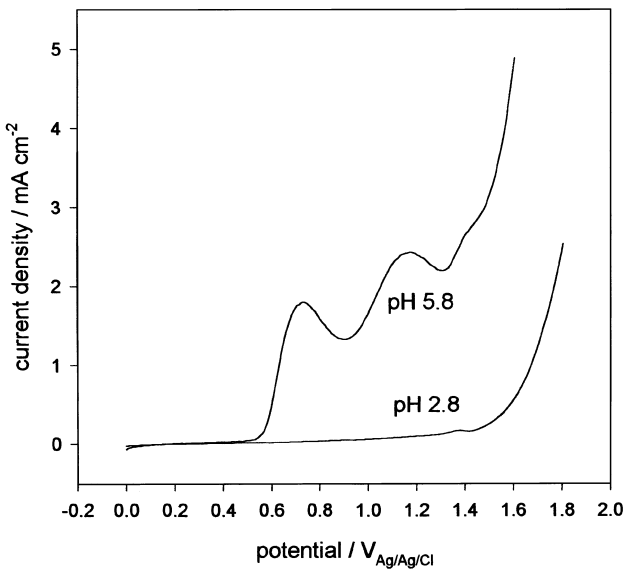


*Fig. 4.* Potentiodynamic curves recorded for Au–Pd–In alloy in 0.5 M $Na_2SO_4$ solution (pH 5.8) and in the same solution adjusted to pH 2.3. Potential sweep rate 20 mV $s^{-1}$.

The EQCM measurements in Figure 5 provided the additional evidence concerning Reaction 3. It is obvious that the electrode mass increases above about 0.65 V indicating accumulation of PdO on the electrode surface. During the reverse potential scan the mass increase ceases at about 0.85 V and below this value the mass remains actually constant. Such an irreversible behaviour implies that cathodic decomposition of PdO does not take place, that is, the oxide layer is passive within the studied potential region. Analogous irreversible passivation was observed using EQCM for copper and titanium electrodes [14].

The resistance of passive metals to corrosion is usually evaluated on the basis of the breakdown potential, at which destruction of the passive layer begins. However, the appearance of the anodic current for Au–Pd–In in the chloride containing solution has another origin: the current is produced by gold dissolution due to complexing by chloride. In other words, the onset of the anodic current during potential sweep indicates the exceeding of the equilibrium potential $E°(Au/AuCl_4^-)$ but not the breakdown potential, which reflects the anticorrosive properties of alloy. Hence, contrary to [2, 3], we conclude that the potentiodynamic transition from a passive state to active dissolution does not provide real criteria about the corrosion resistance of gold-based alloys in solutions containing chloride.

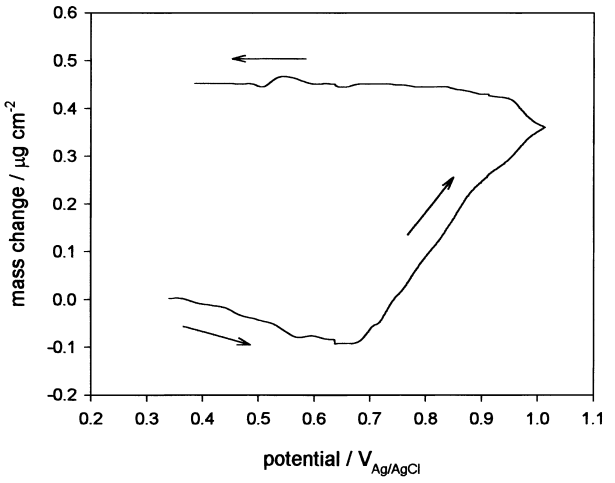


*Fig. 5.* EQCM data for Au–Pd–In alloy in 0.5 $Na_2SO_4$ (pH 5.8) at $v = 10$ mV $s^{-1}$.

### 3.2. *EQCM investigations*

Au–Pd–In alloy was deposited on quartz crystals by means of a magnetron-sputtering (MS) technique and chemical composition of the deposit was determined by X-ray photoelectron spectroscopy (XPS) using surface sputtering by ionised argon. The results of the analysis are given in Table 1. Obviously, the composition of the Au–Pd–In coating corresponds well to the target composition.

Figure 6 shows XRD patterns for cast Au–Pd–In alloy and for that sputtered on quartz substrate. The X-ray reflections indicate that both samples were crystalline. The main phase in both samples was a substitution alloy of palladium and indium in gold. The XRD pattern of the deposit on quartz had some additional peaks (3.26, 1.662 and 1.312 Å), which indicated that the sputtered alloy contained at lest one phase more than the cast alloy. The sputtered deposit had a strong texture in ⟨1 1 1⟩ direction, while crystallites in the casting alloy were randomly orientated. The XRD peaks were broad and this was indicative of ideally imperfect crystallites or the inhomogeneity of alloys.

The electrochemical behaviour of sputtered and cast alloys was investigated previously by using electrochemical impedance spectroscopy (EIS) and potentiodynamic polarization measurements [7]. It was shown that impedance spectra as well as voltammetric curves were

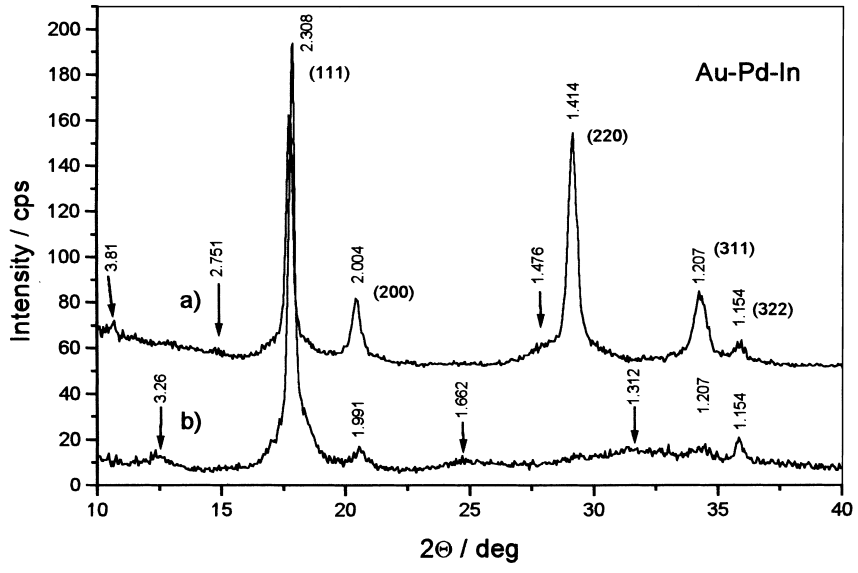


*Fig. 6.* XRD patterns for casting Au–Pd–In alloy (a) and magnetron sputtered one (b) on quartz. Mo$K_\alpha$ radiation.

of similar shape for both alloys, which implied similar electrochemical and corrosive behaviour. Only a difference in actual geometric areas was concluded from the difference in double layer capacities. This difference is understandable when taking into account the different kinds of surface treatment applied (sputtering and mechanical polishing). Hence, the experiments using XPS, XRD, EIS and d.c.-voltammetry showed that both casting and sputtered alloys had similar chemical composition, crystalline structure, and exhibited similar electrochemical behaviour. It can therefore, be, concluded that MS is a suitable tool for preparation of the EQCM sensors for gold-based alloys.

Figure 7 shows the EQCM and the open circuit potential ($E_{ocp}$) data obtained after sample immersion in oxygenated (curve 1) and deoxygenated (curve 2) artificial saliva. In the oxygen free solution a slight increase in the electrode mass ($dm/dt \approx 0.2\,ng\,s^{-1}\,cm^{-2}$) and a positive $E_{ocp}$ shift was observed. The mass increase is due to alloy oxidation by water and accumulation of corrosion products (oxides, hydroxides) on the surface. However, alongside corrosion, some minor contributions of other phenomena are also possible, such as surface roughening and hydration of oxides etc. The corrosion process is associated mainly with indium oxidation, the content of which in the alloy is 6.7% (Table 1). (To be exact, there is also 0.93% of gallium, which also represents a corroding component.) The most likely oxidizing reaction is [15]:°

$$2\,In + 3\,H_2O \rightarrow In_2O_3 + 6\,H^+ + 6\,e^-, \qquad E° = -0.190\,V_{H/H^+} - 0.0591\,pH \quad (5)$$

The solution was saturated with oxygen following about 1 h of electrode immersion in deoxygenated artificial saliva (curve 2, Figure 7). The oxygen introduction manifested itself in the decrease of the $dm/dt$ slope, as well as in the positive $E_{ocp}$ shift. Both effects are indicative of the increase in electrode passivity. Thus, dissolved oxygen did not accelerate the alloy corrosion. On the contrary, the corrosion rate became even lower during solution saturation with oxygen. This behaviour implied a highly passive surface, which developed as a result of Reaction 5.

After electrode immersion in the oxygen pre-saturated artificial saliva, a sharp increase in the electrode mass ($dm/dt \approx 5\,ng\,s^{-1}\,cm^{-2}$) was observed (curve 1,

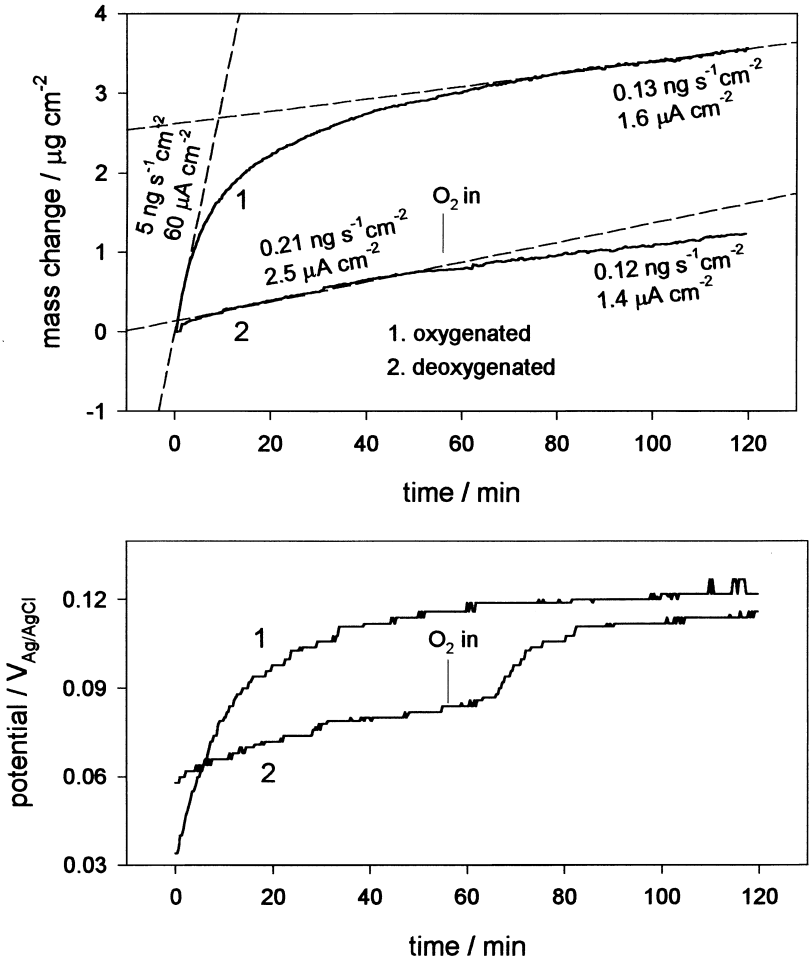


*Fig. 7.* EQCM and $E_{ocp}$ data for Au–Pd–In immersed in oxygen-saturated (1) and deoxygenated (2) artificial saliva. The beginning of solution saturation by oxygen is indicated on curve 2. On curves are given mass change rates (ng $s^{-1}$ $cm^{-2}$) and corrosion current densities ($\mu$A $cm^{-2}$) calculated according to the ratio (Equation 7).

Figure 7). The mass change became rectilinear within 1 h and has slope $dm/dt = 0.13\,ng\,s^{-1}\,cm^{-2}$. The electrode potential changed accordingly: a significant increase in $E_{ocp}$ was observed in the first immersion stages and a steady state value is established in about 1 h. Obviously, the initial electrode surface was rather active and became passive during corrosion because of the development of a protective layer. The mass of the protective layer ($m_{pl}$) may be estimated as follows:

$$m_{pl} = \Delta m_{O_2} - \Delta m_{Ar} \quad (6)$$

where $\Delta m_{O_2}$ and $\Delta m_{Ar}$ is the absolute mass gain at a given time interval in the oxygenated and oxygen-free solution, respectively. For instance, we can estimate from Figure 7 that the mass of the layer is $m_{pl} \approx 2.2\,\mu g\,cm^{-2}$ following 1 h immersion in the oxygen saturated solution.

Corrosion rates can be estimated according to the ratio [16–18]:

$$j_{corr} = \pm\left(\frac{nFC}{\Delta M}\right)\left(\frac{df}{dt}\right) \quad (7)$$

where $j_{corr}$ is the corrosion current density (A $cm^{-2}$), $df/dt$ is the rate of the change of quartz oscillation frequency, $F$ is the faradaic constant, $n$ is the number of electrons in the corrosion reaction, $\Delta M$ is the molar mass of the group responsible for the mass gain during corrosion (O, OH, OOH etc.), and $C$ is the proportional coefficient between the frequency and mass change (according to Sauerbrey's equation [19], $C = 18$ ng $Hz^{-1}$ $cm^{-2}$ when the main resonance frequency is $f_0 = 5$ MHz). If the metal is dissolved and transferred to the solution, the parameter $\Delta M$ has the meaning of molar mass of metal (the corroding alloy component) [15].

In the case of $dm/dt = 1\,ng\,s^{-1}\,cm^{-2}$ and $f_0 = 5\,MHz$, the ratio (Equation 7) is simplified to

$$j_{corr} = \frac{9.65 \times 10^{-5} n}{\Delta M} \quad (8)$$

The $j_{corr}$ values calculated according to Equation 8 for different scarcely soluble compounds are given in Table 2. It is noteworthy that because of the same ratio $n/\Delta M$ different oxides ($Me_2O$, MeO, $Me_2O_3$) give the same $j_{corr}$ value. Thus, if oxide formation is prevailing, the estimation of corrosion current density does not require the exact knowledge, as to which oxide forms during corrosion. The hydroxides ($Me(OH)_3$, MeOOH),

*Table 2.* $j_{corr}$ values calculated at $dm/dt = 1\,ng\,s^{-1}$ according to Equation 7 assuming accumulation of different scarcely soluble compounds on corroding surface

| Compound | $MeO_2$ | $Me_2O$ | MeO | $Me_2O_3$ | $Me(OH)_3$ | MeOOH |
|---|---|---|---|---|---|---|
| Corrosion current density /$\mu$A $cm^{-2}$ | 12 | 12 | 12 | 12 | 5.68 | 5.8 |

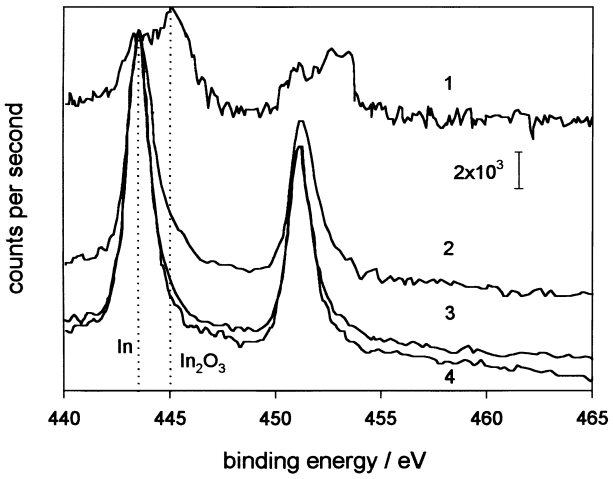


*Fig. 8.* XPS spectra recorded for Au–Pd–In coating deposited by magnetron sputtering after immersion for 2 h in naturally aerated 0.9 M NaCl solution. Surface sputtering time by ionized argon: (1) 0, (2) 30, (3) 60 and (4) 120 s.

however, yield around twice lower corrosion current densities than those of the oxides (Table 2). Thus, the maximum error in $j_{corr}$ estimation (without knowledge of surface layer composition) is about 100%. Of course, exact corrosion current calculations require surface layer composition definition using analytical techniques.

The XPS spectra indicated $In_2O_3$ ($E_b = 444.7 \pm 0.2$ eV) or/and $In(OH)_3$ ($E_b = 445 \pm 0.7$ eV [9, 10]) on the specimen surface (Figure 8). According to [15], $In(OH)_3$ is less stable than $In_2O_3$ and tends to be converted into the oxide. Hence, assuming $In_2O_3$ as a corrosion product, the calculated corrosion rate in deoxygenated artificial saliva is as high as $j_{corr} = 2.5\,\mu A\,cm^{-2}$ ($dm/dt = 0.21\,ng\,s^{-1}\,cm^{-2}$, curve 2, Figure 7). Analogously, the initial corrosion rate in the oxygen saturated solution is $j_{corr} = 60\,\mu A\,cm^{-2}$. The steady state corrosion rate in the same solution established after 1–2 h is $j_{corr} = 1.6\,\mu A\,cm^{-2}$.

The results of the EQCM investigations in the acid solution containing lactic acid (Figure 9) are qualitatively similar to those obtained in almost neutral artificial saliva (Figure 7). The initial mass gain in the oxygen-saturated solution yields the corrosion rate $j_{corr} = 84\,\mu A\,cm^{-2}$ (Figure 9). This rate is somewhat higher than that determined in artificial saliva. The mass of the protective layer developed after 1 h immersion in the oxygenated lactic acid solution is also higher compared to that of artificial saliva (4 and 2.2 $\mu g\ cm^{-2}$, respectively). Thus, the initial corrosion rates in lactic acid solution are higher than those in artificial saliva. With the immersion time, however, the corrosion rates become similar in both solutions (2.2 $\mu A\ cm^{-2}$ in lactic acid and 1.6 $\mu A\ cm^{-2}$ in artificial saliva).

The mass curve obtained in the oxygenated NaCl solution (Figure 10) is very similar to that in the lactic acid solution (Figure 9). This implies that dissolution of corrosion products in both solutions was negligible. It seems unlikely that the mass gain in acid solution would be the same as in neutral if such dissolution took place.

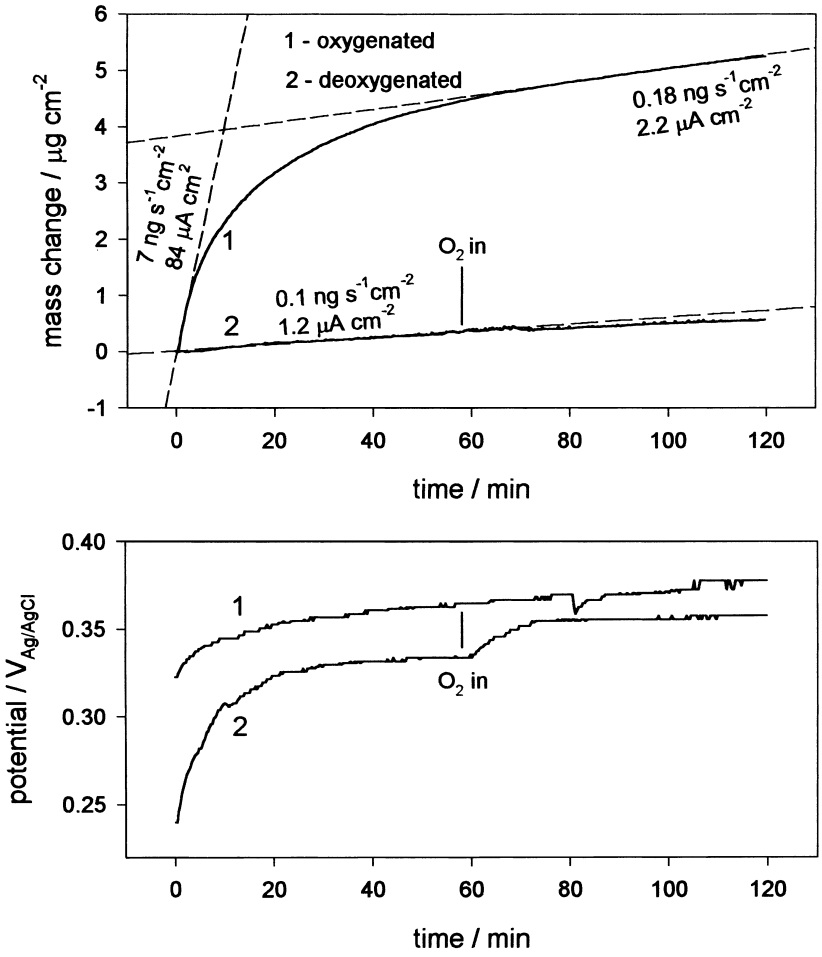


*Fig. 9.* EQCM and $E_{ocp}$ data for Au–Pd–In immersed in oxygen-saturated (1) and deoxygenated (2) solution containing 0.1 M NaCl and 0.1 M lactic acid. Mass change rates (ng $s^{-1}$ $cm^{-2}$) and corrosion current densities ($\mu$A $cm^{-2}$) calculated according to the ratio (Equation 7) given on curves. Beginning of solution saturation by oxygen as indicated on curve 2.

An attempt has been made to determine the Au–Pd–In corrosion rate in the oxygenated lactic acid solution using voltammetric measurements (Figure 11). The $E$–log($j$) dependencies obtained have a rather complicated shape. The entire cathodic curve is most likely the sum of partial currents of oxygen, free proton, water decomposition and metal ions, minor amounts of which are always present in the vicinity of electrode. As a result, extrapolation of the rectilinear part of the cathodic dependence to $E_{ocp}$ gives a much higher value than extrapolation of the anodic dependence. The anodic curve is complicated by the contribution of gold dissolution leading to the current peak discussed above. The most reliable part for the corrosion rate evaluation seems to be in the region 0.4–0.6 V. The latter gives the corrosion rate $j_{corr} \approx 4\,\mu A\,cm^{-2}$ (Figure 11). This result is comparable with the value $j_{corr} = 2.2\,\mu A\,cm^{-2}$ obtained from the EQCM measurements (Figure 9).

## 4. Conclusions

The electrochemical quartz crystal nanobalance (EQCM) has been applied to corrosion studies of Au–Pd–In alloy in simulated physiological solutions. The alloy was coated on quartz crystals by means of a magnetron-sputtering (MS) technique. Investigations by X-ray photoelectron spectroscopy (XPS) and surface sputtering by ionised argon showed that the composition of Au–Pd–In coatings corresponded well to the MS target composition. The X-ray diffraction measurements revealed the crystalline structure of the sputtered deposits.

The EQCM reflected sensitively the alloy corrosion dynamics in both deoxygenated and oxygen-saturated solutions. Corrosion resulted in an electrode mass increase due to the accumulation of sparingly soluble corrosion products on the corroding surface. The XPS analysis showed $In_2O_3$ to be the main corrosion product on the surface. The mass gain in neutral NaCl solution was not greater than that in lactic acid solution (pH 2.2). This implied that dissolution of corrosion products in both solutions was negligible.

It was demonstrated that potentiodynamic transition from the passive state to active dissolution failed to provide the information about corrosion resistance of gold-based alloys in simulated physiological solutions. Such transition should be attributed rather to gold

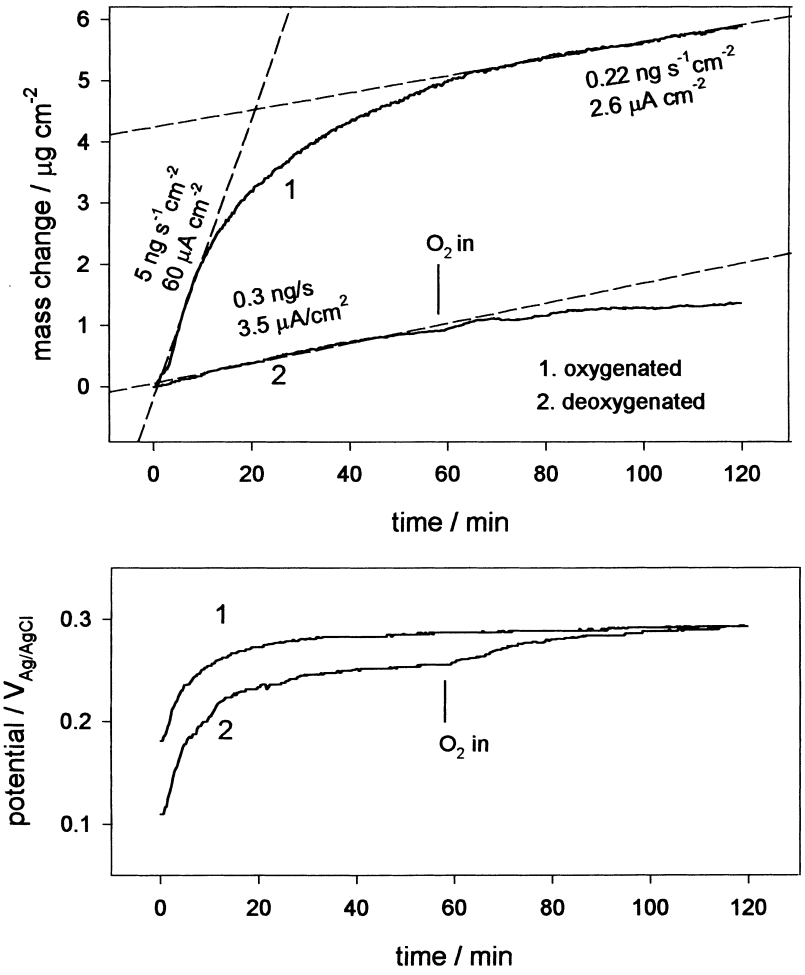


*Fig. 10.* EQCM and $E_{ocp}$ data for Au–Pd–In immersed in oxygen-saturated (1) and deoxygenated (2) 0.9 M NaCl. On curves are given mass change rates (ng $s^{-1}$ $cm^{-2}$) and corrosion current densities ($\mu$A $cm^{-2}$) calculated according to the ratio (Equation 7). Beginning of solution saturation by oxygen as indicated on curve 2.

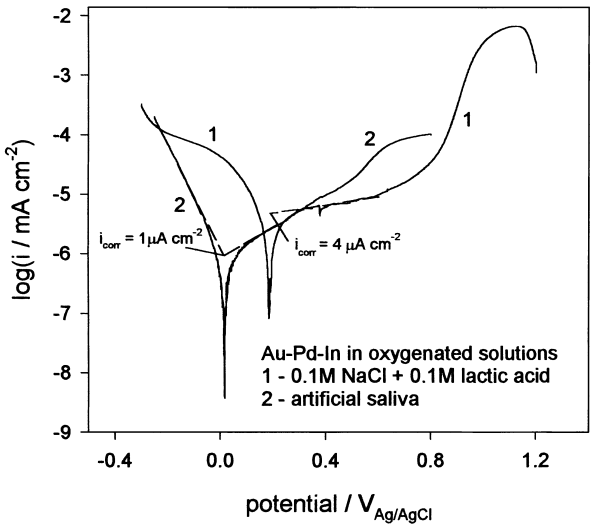


*Fig. 11.* Potentiodynamic curves obtained at $v = 5$ mV $s^{-1}$ for Au–Pd–In immersed in oxygen-saturated 0.1 M NaCl + 0.1 M lactic acid (curve 1) and artificial saliva (curve 2). Measurements were performed following the EQCM measurements (curves 1 in Figures 9 and 12).

dissolution and chloride complex formation than to the breakdown of any passive layer.

## Acknowledgement

This work was supported by the Lithuanian Science Foundation (Contract 365, 1999).

## References

1. H. Hamanaka and T. Yoneyama, *Corros. Eng.* **38** (1989) 373.
2. J.-M. Meyer and L. Reclaru, *J. Mater. Sci., Mater. Med.* **6** (1995) 534.
3. G. Hilderbrand, D. Kraft, K. Liefeith, E. Mann and E. Lenz, *Werkst. Korros.* **46** (1995) 157.
4. R.F. Sandenbergh, *Gold 100. Vol. 3:* Proceedings of the symposium on the 'Industrial Uses of Gold'. Johannesburg, SAIMM 45 (1986).
5. R.A. Silva, M.A. Barbosa, R. Vilar, O. Conde, M. Da Cunha Belo and I. Sutherland, *J. Mater Sci., Mater. Med.* **5** (1994) 353.
6. T.-P. Cheng, W.T. Tsai, J.-H. Chern Lin and J.-T. Lee, *J. Mater. Sci., Mater. Med.* **1** (1990) 211.
7. K. Leinartas, M. Samulevičienė, A. Sudavičius, V. Lisauskas, B. Vengalis and E. Juzeliūnas, *Corros. Sci.*, (submitted).
8. R. Butkutė, PhD thesis. Semiconductor Physics Institute, Vilnius (1998).
9. C.D. Wagner, W.M. Riggs, L.E. Davis, J.F. Moulder and G.E. Muilenberg. 'Handbook of X-ray Photoelectron Spectroscopy' (Perkin Elmer, Minnesota, 1978), p. 190.

10. D. Briggs and M.P. Seach (Eds), Practical Surface Analysis by Auger and X-ray Photoelectron Spectroscopy (J. Wiley & Sons, New York, 1983).
11. E. Juzeliūnas, P. Kalinauskas and P. Miečinskas, *J. Electrochem. Soc*. **143** (1996) 1525.
12. D. Jelinskienė, K. Leinartas and E. Juzeliūnas, *Chemija* **11**(4) (2000) 165.
13. A.I. Bard (Ed), '*Encyclopedia of Electrochemistry of Elements*' Vol. 4 (1976), p. 207.
14. R. Schumacher, *Angew. Chem*. **102** (1990) 347.
15. M. Pourbaix, 'Atlas of Electrochemical Equilibria in Aqueous Solutions' (Cebelcor, Brussels, 1966), p. 436.
16. E. Juzeliūnas, *Elektrokhimiya* **28** (1992) 1656.
17. A. Leng, Diploma thesis, University Düsseldorf (1991).
18. M. Stratmann, W. Fürbeth, G. Grundmeier, R. Lösch and C.R. Reinartz, Corrosion Inhibition by Adsorbed Monolayers, *in* P. Markus and J. Oudar (Eds), 'Corrosion Mechanisms in Theory and Practice' (Marcel Dekker, New York 1995), p. 401.
19. G. Sauerbrey, *Z. Phys*. **155** (1959) 206.